DOI: 10.1002/chem.201001654

A Photoelectrochemical Immunosensor Based on Au-Doped TiO_2 Nanotube Arrays for the Detection of α-Synuclein

Yarui An,[a] Linlin Tang,[a] Xiaoli Jiang,[a] Hua Chen,[a] Meicheng Yang,[a] Litong Jin,[a] Shengping Zhang,[b] Chuangui Wang,[b] and Wen Zhang*[a]

Abstract: α-Synuclein (α-SYN) is a very important neuronal protein that is associated with Parkinson's disease. In this paper, we utilized Au-doped TiO_2 nanotube arrays to design a photoelectrochemical immunosensor for the detection of α-SYN. The highly ordered TiO_2 nanotubes were fabricated by using an electrochemical anodization technique on pure Ti foil. After that, a photoelectrochemical deposition method was exploited to modify the resulting nanotubes with Au nanoparticles, which have been demonstrated to facilitate the improvement of photocurrent responses. Moreover, the Au-doped TiO_2 nanotubes formed effective antibody immobilization arrays and immobilized primary antibodies (Ab_1) with high stability and bioactivity to bind target α-SYN. The enhanced sensitivity was obtained by using {Ab_2-Au-GOx} bioconjugates, which featured secondary antibody (Ab_2) and glucose oxidase (GOx) labels linked to Au nanoparticles for signal amplification. The GOx enzyme immobilized on the prepared immunosensor could catalyze glucose in the detection solution to produce H_2O_2, which acted as a sacrificial electron donor to scavenge the photogenerated holes in the valence band of TiO_2 nanotubes upon irradiation of the other side of the Ti foil and led to a prompt photocurrent. The photocurrents were proportional to the α-SYN concentrations, and the linear range of the developed immunosensor was from 50 $pg\,mL^{-1}$ to 100 $ng\,mL^{-1}$ with a detection limit of 34 $pg\,mL^{-1}$. The proposed method showed high sensitivity, stability, reproducibility, and could become a promising technique for protein detection.

Keywords: immunoassays · nanotubes · photoelectrochemistry · proteins · sensors

Introduction

Parkinson's disease (PD) is a chronically progressive, age-related neurodegenerative disorder, which is characterized by rest tremor, balance impairment, slowness of movement, and rigidity.[1] Although the main pathological feature of PD is the selective death of dopaminergic neurons in the substantia nigra, the etiology of this common neurodegenerative disease remains to be elucidated.[2] Recently, many researchers have concentrated on the study of the normal and disease-associated functions of α-synuclein (α-SYN), which is an essential neuronal protein probably implicated in PD.[3,4] Some research has indicated that overexpression of mutant and wild-type human α-SYN in mice or flies induces a slowly progressive neurodegenerative phenotype with a late onset.[5,6] Accumulation of soluble α-SYN can render endogenous dopamine toxic, thereby suggesting a potential mechanism for the selectivity of neuronal loss.[7] Several investigators have also reasoned that the quantification of extracellular α-SYN could provide a platform for marker development of human synucleinopathies, including PD.[8] All these facts clearly indicate that α-SYN is an important pathological protein associated with neurodegenerative diseases.[9] Therefore, to clarify the properties and functions of α-SYN, the development of effective methods for quantitative analysis of this protein has tremendous importance in neurological disease etiology study and clinic diagnosis.

Up to now, a variety of strategies have been used for the quantitative detection of α-SYN, including NMR spectroscopy,[10] fluorescence measurements,[11] western blotting,[8] and

[a] Dr. Y. An, L. Tang, X. Jiang, H. Chen, Dr. M. Yang, Prof. L. Jin, Prof. W. Zhang
Department of Chemistry
East China Normal University
Shanghai 200062 (China)
Fax: (+86) 21-6223-2627
E-mail: wzhang@chem.ecnu.edu.cn

[b] Dr. S. Zhang, Prof. C. Wang
Institute of Biomedical Sciences
College of Life Science
East China Normal University
Shanghai 200241 (China)

size-exclusion chromatography (SEC).[12] However, most methods often involve sophisticated instrumentation, and clinically unrealistic expense and time.[13] Immunoassay, with the remarkable development in such fields as biochemical technology, seems to be one of the most popular techniques for bioanalysis based on the selective nature of the recognition between antigen and antibody.[14] One of the traditional immunoassays is enzyme-linked immunosorbent assay (ELISA), which is widely used in clinical and biochemical analysis by enzymatic amplification of the signals.[15–18] To improve the traditional ELISA, electrochemical techniques such as potentiometry,[19] amperometry,[20,21] and conductometry[22] have all been explored with regard to immunoassay development. Among these improved techniques, photoelectrochemical detection, the ultrahigh sensitivity of which is achieved by employing two separate forms of signal for excitation and detection, has become an attractive and promising method for biological assay.[23,24] For instance, CdS quantum dots (QDs) have been developed to form an acetylcholine esterase (AChE)–CdS nanoparticle hybrid system for the photoelectrochemical detection of AChE inhibitors.[25] SnO_2 nanoparticles have been used as electrode material for quantitative detection of a biological affinity reaction, biotin–avidin recognition.[26] Among various semiconductors, TiO_2 is of special interest in the wide application of photoelectrochemistry because it possesses nontoxicity, environmental safety, photochemical stability,[27–29] and in particular, biocompatibility and negligible protein denaturation.[30,31] These properties make TiO_2 an ideal sensing material for electrochemical biosensor design.[28] To the best of our knowledge, no immunosensor has employed TiO_2 nanotubes as a substrate for the determination of proteins in photoelectrochemical bioanalysis.

Herein, we describe the construction of a novel photoelectrochemical immunosensor for α-SYN detection based on Au-doped TiO_2 nanotubes. The highly ordered TiO_2 nanotube arrays were fabricated by the electrochemical anodic oxidation technique. Au nanoparticles were then photoelectrochemically deposited in the TiO_2 nanotubes on both sides of the Ti foil, and the resulting Au-doped TiO_2 nanotubes were proved to facilitate the improvement of the photoelectrochemical performance of semiconductive nanomaterials,[32,33] as well as the immobilization of primary antibodies on nanotubes.[34,35] With the aim of protecting biomolecules from UV irradiation, in the case of the immunoassay protocol, the primary antibody (Ab_1) was just immobilized on one side of Au-TiO_2-modified Ti foil. The analytical procedure consisted of the immunoreaction of target α-SYN with Ab_1, followed by the attachment of {Ab_2-Au-GOx} bioconjugates, which featured secondary antibody (Ab_2) and glucose oxidase (GOx) labels linked to Au nanoparticles, and could afford the assay excellent sensitivity by signal amplification. When this immunosensor was exposed to a solution containing glucose, the GOx that was immobilized on one side of the Ti foil could catalyze the conversion of glucose into gluconic acid and H_2O_2. The latter product acted as a sacrificial electron donor to scavenge the holes generated in the valence band of TiO_2 nanotubes upon irradiation of the other side of the Ti foil, thereby improving the accumulation of electrons and leading to a remarkable photocurrent. The α-SYN concentration, which was proportional to that of the GOx labels linked to Au nanoparticles, could be readily examined through measurement of the photocurrent derived from the photoelectrochemical reaction of H_2O_2. Under optimal conditions, the linear relationship between the photocurrent and α-SYN concentration was obtained in the range of 50 $pg\,mL^{-1}$ to 100 $ng\,mL^{-1}$. The detection limit was estimated to be 34 $pg\,mL^{-1}$, which showed that the fabricated immunosensor exhibited good sensitivity. The results demonstrated that the developed immunosensor supplied a convenient, low-cost, and sensitive method for α-SYN determination. Moreover, the established method could provide an approach for the design of photoelectrochemical immunosensors for analysis of other significant proteins in the future.

Results and Discussion

SEM images of TiO_2 and Au-TiO_2 nanotubes: Figure 1 shows the SEM images of the TiO_2 nanotubes used in this work. It is observed that high-density, well-ordered, and uniform TiO_2 nanotubes of about 75 nm in diameter were fabricated on the pure Ti foil with the electrochemical anodic oxidation technique (Figure 1a). In Figure 1b, it is clearly shown that Au nanoparticles (arrows) were deposited in the nanotubes, and that the diameter of the nanoparticles ranged from 40 to 50 nm. The Au nanoparticles were not aggregated, which indicates that the photoelectrochemical deposition method compares favorably to the conventional photodeposition technique (Figure 1c).

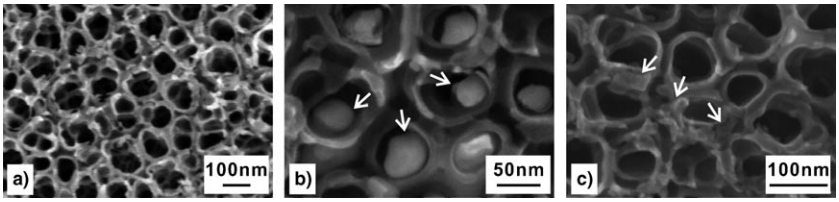

Figure 1. Morphologies of TiO_2 nanotubes: a) a typical SEM image of well-ordered TiO_2 nanotubes; and SEM images of Au-doped TiO_2 nanotubes prepared by using b) a photoelectrochemical deposition method and c) a photodeposition method.

Electrochemical characteristics of the TiO_2 surface: It is well known that electrochemical impedance spectroscopy (EIS) is an effective and convenient method for probing the

features of a modified electrode surface. Each reaction step of the modified electrode was analyzed by EIS in the frequency range $0.1–1.0\times10^5$ Hz, and in a phosphate buffer solution (PBS; 0.01 M, pH 7.4) containing $[Fe(CN)_6]^{3-}$/$[Fe(CN)_6]^{4-}$ (1:1, 2.5 mM) as probe. Figure 2 represents the

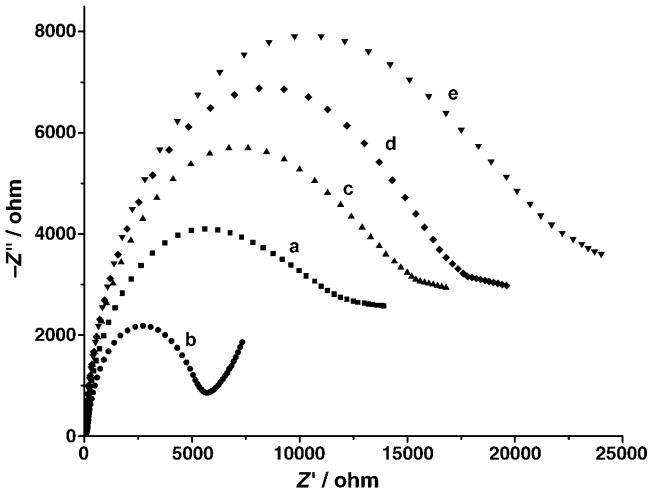

Figure 2. Nyquist plots of the electrochemical impedance spectroscopy (EIS) for different electrodes: a) TiO_2, b) TiO_2-Au, c) TiO_2-Au-Ab_1, d) TiO_2-Au-Ab_1-α-SYN, e) Au-TiO_2-Au-Ab_1-α-SYN-{Ab_2-Au-GOx},- which were measured in PBS (pH 7.4) containing $[Fe(CN)_6]^{3-}$/$[Fe(CN)_6]^{4-}$ (1:1, 2.5 mM).

Nyquist plots for the TiO_2 electrode, TiO_2-Au electrode, TiO_2-Au-Ab_1 electrode, TiO_2-Au-Ab_1-α-SYN electrode, as well as the TiO_2-Au-Ab_1-α-SYN-{Ab_2-Au-GOx} electrode. At the TiO_2 electrode (Figure 2a), the redox process of the $[Fe(CN)_6]^{3-/4-}$ probe showed a high electron-transfer resistance. The TiO_2-Au electrode showed a much lower resistance for the redox probe (Figure 2b), which implies that the Au nanoparticles greatly accelerated the electron transfer, which demonstrates that the Au nanoparticles had been successfully deposited in the TiO_2 nanotubes. When primary antibodies (Ab_1) were adsorbed onto the TiO_2-Au electrode, the curve increased notably (Figure 2c). Further binding of α-SYN retarded the interfacial electron transfer of the $[Fe(CN)_6]^{3-/4-}$ pair, which provided evidence of the successful formation of the immunocomplex (Figure 2d). In the final step, the attachment of {Ab_2-Au-GOx} bioconjugates gave rise to an additional barrier towards the access of the redox probe to the electrode, which resulted in a further increase in the electrode-transfer resistance (Figure 2e).

Characterization of Au nanoparticles and {Ab_2-Au-GOx} bioconjugates: The interaction between Au nanoparticles and GOx and Ab_2 was demonstrated with UV-visible absorption spectroscopy. Figure 3a and b show the absorption spectra of the dispersed Au nanoparticles, and the mixture of GOx and Ab_2, respectively. Au nanoparticles exhibited a typical characteristic of the surface plasmon band at approximately 520 nm. The characteristic peak of GOx and Ab_2 appeared at 280 nm, which corresponds to the π–π* transition

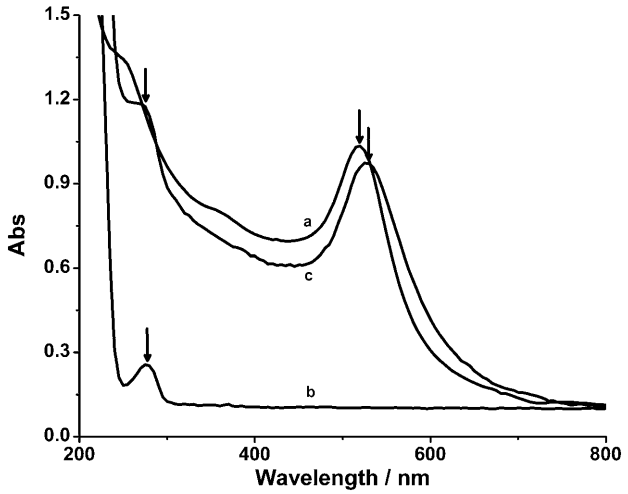

Figure 3. UV-visible absorption spectra of a) the gold nanoparticles, b) the mixture of GOx and Ab_2, and c) {Ab_2-Au-GOx} bioconjugates.

in the tryptophan and tyrosine residues of the proteins.[36] After Au nanoparticles had been modified with GOx and Ab_2, several absorption peaks were simultaneously observed in comparison with that of pure Au nanoparticles (Figure 3c). The peak at 269 nm was mainly ascribed to GOx and Ab_2 in contrast with that of pure GOx and Ab_2. Additionally, a remarkable shift of the absorption band toward a higher wavelength (530 nm) along with further broadening of the absorption band was observed, which suggests that GOx and Ab_2 could be bound to the Au nanoparticles to yield {Ab_2-Au-GOx} bioconjugates.[37,38]

The morphologies and microstructures of the pure Au nanoparticles and modified Au nanoparticles were also confirmed by TEM images. As shown in Figure 4a, a homogeneous dispersion of Au nanoparticles with a mean diameter of 18 nm could be observed. After the Au nanoparticles had

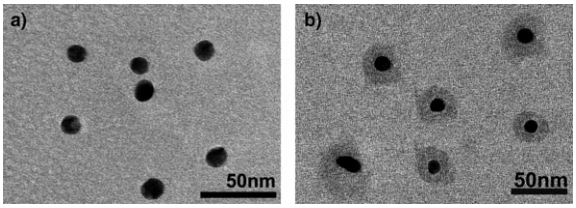

Figure 4. TEM images of a) gold nanoparticles and b) {Ab_2-Au-GOx} bioconjugates.

been modified with GOx and Ab_2, they increased in diameter, and the edge of the conjugated nanoparticles had a gray halo (Figure 4b), which visually demonstrated that GOx and Ab_2 had been loaded onto the Au nanoparticles to yield the {Ab_2-Au-GOx} bioconjugates. These results completely agree with those from UV-visible absorption spectroscopy.

Detection mechanism of the photoelectrochemical immunosensor: The detailed mechanism of the photoelectrochemical detection is illustrated in Scheme 1g. When the TiO_2-Au-

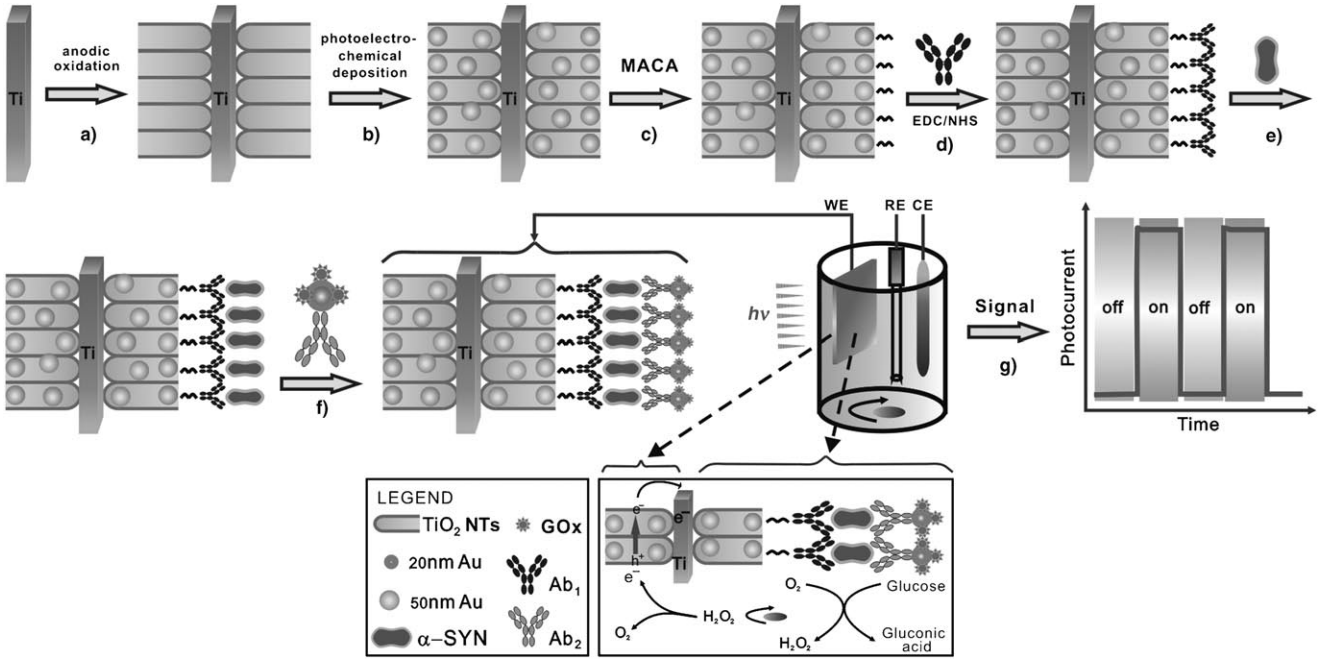

Scheme 1. Procedure for the synthesis of the TiO_2-Au-Ab_1-α-SYN-{Ab_2-Au-GOx} immunosensor and the mechanism for the photoelectrochemical detection of α-SYN.

Ab_1-α-SYN-{Ab_2-Au-GOx} immunosensor was exposed to a detection solution containing glucose, the GOx immobilized on one side of the Ti foil could catalyze the conversion of glucose into gluconic acid and H_2O_2. The latter product, upon irradiation of Au-TiO_2 on the other side of the Ti foil, acted as a sacrificial electron donor to deplete the photogenerated holes located on the electrode, and improves the efficiency of charge separation. A greater amount of GOx immobilized on the immunosensor can lead to a higher yield of electron donor H_2O_2.[39] Then, the scavenging of valence-band holes is enhanced and as a result, the photocurrent is increased. The α-SYN concentration, which is proportional to that of the GOx labels, can be readily examined through the measurement of the photocurrent derived from the photoelectrochemical reaction of H_2O_2.

Effect of Au nanoparticles in TiO_2 on photocurrent response: Two types of Au-doped TiO_2 nanotube immunosensors were designed to evaluate the effect of Au nanoparticles on photocurrent responses (Figure 5). Single-sided and double-sided Au-doped TiO_2 nanotube immunosensors are denoted in the following as S-Au-TiO_2 and D-Au-TiO_2, respectively. The photocurrents generated from the immunosensors were measured for their response towards α-SYN (20 ng mL^{-1}) in the absence and presence of glucose (40 μM) at room temperature. In the absence of glucose, the D-Au-TiO_2 immunosensor exhibited a stronger photocurrent response than that of S-Au-TiO_2 (Figure 5b and a), which was of special relevance to Au nanoparticle deposition. The presence of Au nanoparticles has been proven to promote charge separation within the TiO_2 nanostructures, as well as interfacial hole

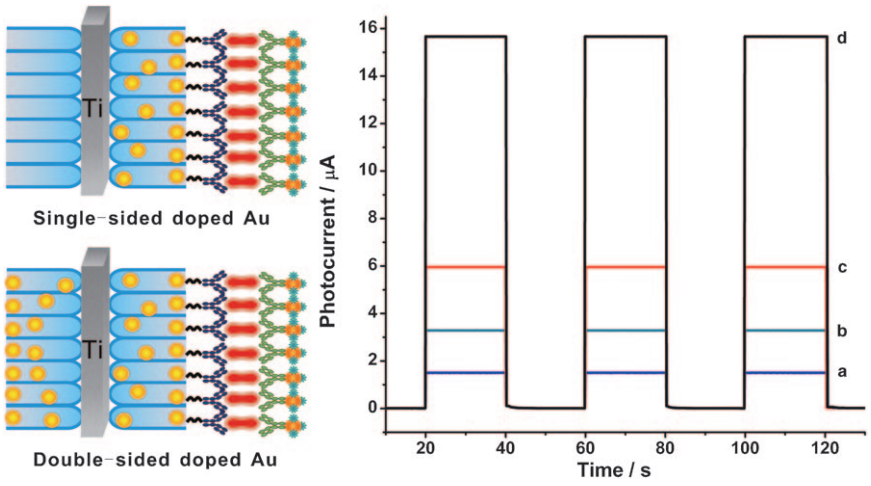

Figure 5. Photocurrent response of S-Au-TiO_2 and D-Au-TiO_2 immunosensors in the absence of glucose (a and b, respectively) and after the addition of 40 μM glucose (c and d, respectively). Data were recorded at a potential of 0.6 V in PBS (0.05 M, pH 7.0) under illumination with light of 365 nm.

transfer.[32–33] When an efficient electron donor (H_2O_2) is in the solution, the electron–hole recombination is restrained and the photocurrent can be enhanced. The addition of glucose (40 μM), an enzyme substrate, led to an increased photocurrent in both of the S-Au-TiO_2 and D-Au-TiO_2 immunosensors (Figure 5c and d). The photocurrent observed in D-Au-TiO_2 was enhanced approximately threefold relative to S-Au-TiO_2. The results showed that D-Au-TiO_2 exhibited a stronger response to glucose than S-Au-TiO_2, which strongly confirmed the principal role of Au nanoparticles in improving the performance of the photoelectrochemical immunosensor.

Effect of applied potential and enzyme-catalyzed reaction time on photocurrent response: The applied potential is an important factor relevant to the photocurrent response. As seen in Figure 6, with the increments of applied potential, the photocurrent was enhanced and leveled off at 0.6 V (Figure 6a). This indicated that the photogenerated electrons were effectively driven to the counter electrode by the positive potential, which could be beneficial to charge separation. Therefore, 0.6 V was selected as the applied potential for the photoelectrochemical experiments in this study.

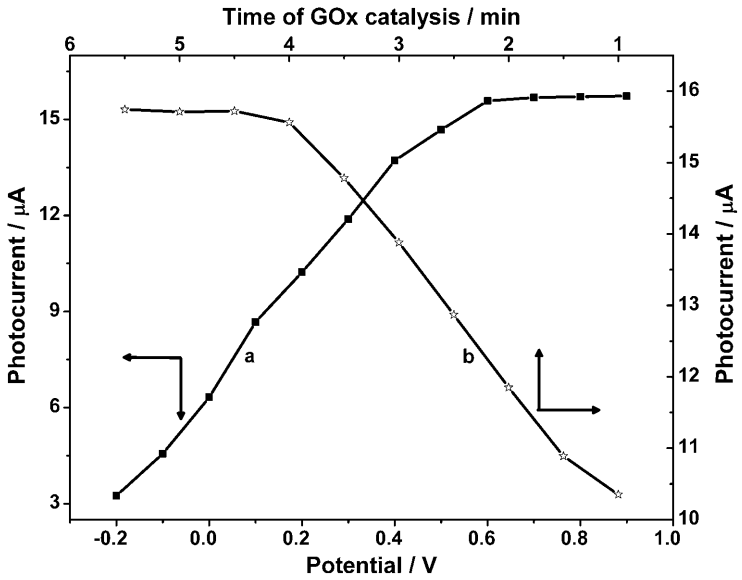

Figure 6. Influence of the applied potential and effect of the time of GOx catalysis on the photoelectrochemical response of the immunosensor to 20 ng mL^{-1} α-SYN.

The length of the enzyme-catalyzed reaction time also greatly affects the amount of H_2O_2 generated, which is relative to the photocurrent response. When the reaction time ranged from 1 to 5.5 min, the photocurrent response increased and then reached a plateau at 4 min (Figure 6b). This could be explained by the fact that with the increase of enzyme-catalyzed reaction time, GOx immobilized on the immunosensor could catalyze glucose to produce more H_2O_2, which acted as a sacrificial electron donor to scavenge the holes. Hence, electron–hole recombination was inhibited and the photocurrent response could be enhanced. Thus, 4 min was selected as the optimum time for the enzyme-catalyzed reaction in this study.

Optimization of experimental conditions: In the sandwich-type immunoassays, temperature and time for the antigen–antibody interaction greatly influence the sensitivity of the developed immunosensor. Figure 7a shows the effect of immunochemical incubation (i.e., when antigen–antibody reaction occurs) temperature on the photocurrent response in the range from 10 to 50 °C. The maximum response occurred at 37 °C, whereas temperatures over 37 °C resulted in a deterioration of the photocurrent response. The reason for this may be that the high temperature caused an irreversible re-

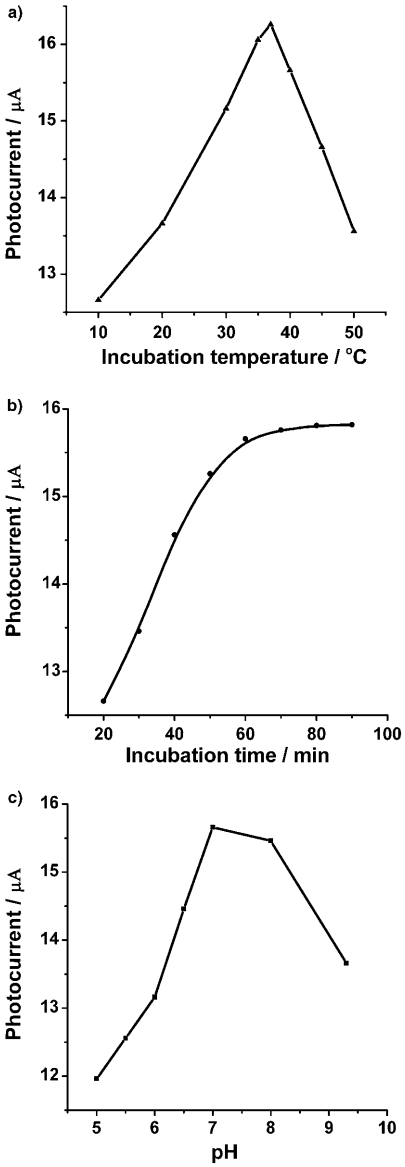

Figure 7. Effects of a) incubation temperature, b) incubation time, and c) pH of the detection solution on the photocurrent response of the TiO_2-Au-Ab_1-α-SYN-{Ab_2-Au-GOx} immunosensor toward 20 ng mL^{-1} α-SYN in 0.05 M PBS containing 40 μM glucose.

action to occur (denaturation of glucose oxidase) and thus affect the process. Additionally, temperatures lower than 37 °C could reduce the immunoreaction rate, thus lengthening the incubation time. Consequently, the temperature of 37 °C was selected for further studies.

At the optimized temperature, the photocurrent response increased with incubation time and reached a plateau at 60 min (Figure 7b). An incubation time longer than this did not clearly improve the response. Therefore, subsequent experiments employed 60 min as the optimum time for all the incubation steps of the assay.

The pH value of the detection solution was also investigated in the enzymatic response. The pH can influence the activity of Ab_1, α-SYN, Ab_2, as well as GOx labels immobilized on the immunosensor surface. As seen in Figure 7c, the immunosensor showed an optimal photocurrent response at pH 7.0. Therefore, PBS with a pH of 7.0 was used as the detection solution for the photoelectrochemical immunoassay.

Reproducibility and stability of the photoelectrochemical immunosensor: The repeatability and reproducibility of the proposed immunosensor were assessed by assaying α-SYN at three levels for five repeat measurements, and the mean current responses are listed in Table 1. The relative standard deviation (R.S.D.) values were estimated as 2.5, 1.9, and 1.5% at 0.1, 1.0, and 10 ng mL^{-1} α-SYN, respectively. The results suggest that the reproducibility of the TiO_2-Au-Ab_1-α-SYN-{Ab_2-Au-GOx} immunosensor was satisfactory.

Table 1. Reproducibility of the photoelectrochemical immunosensor.

$C_{\alpha\text{-SYN}}$ [ng mL^{-1}]	I [μA][a]	R.S.D. [%]
0.1	0.105	2.5
1.0	0.963	1.9
10	11.05	1.5

[a] The mean value of five assays.

The regeneration of the immunosensor was investigated by rinsing it with a stripping buffer, namely, pH 2.8 Gly-HCl solution, to dissociate the antigen–antibody complex. The renewed immunosensor could restore 96.2% of the initial photocurrent after five cycles, which is indicative of high reusability and stability.

Figure 8 shows the stability of the photocurrent response of Au-TiO_2 nanotubes. The photocurrent responses were recorded as the excitation light was turned on and off. The irradiation process was repeated more than 30 times over 20 min, and the photocurrent was very stable over this time without any noticeable decrease. The long-term stability of this immunosensor was also examined. When the immunosensor was stored in pH 7.4 PBS at 4 °C, it retained 96.1% of its initial photocurrent response to 40 ng mL^{-1} α-SYN after a storage period of seven days.

Photoelectrochemical response of iummunosensor to α-SYN concentration: Figure 9A depicts the typical time-based photocurrent response of the photoelectrochemical

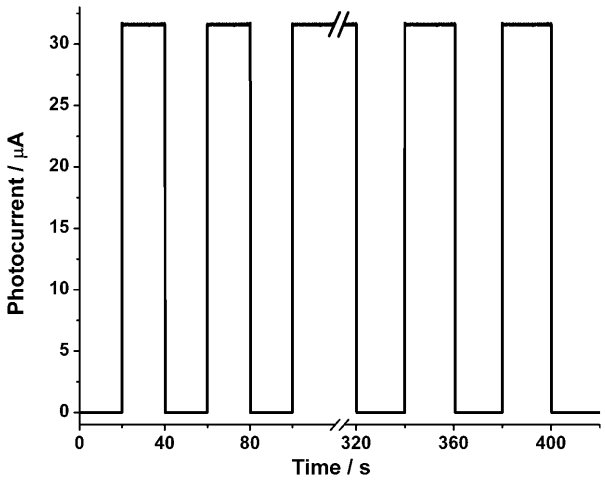

Figure 8. The time-based photocurrent response of the TiO_2-Au-Ab_1-α-SYN-{Ab_2-Au-GOx} immunosensor in 7.0 PBS.

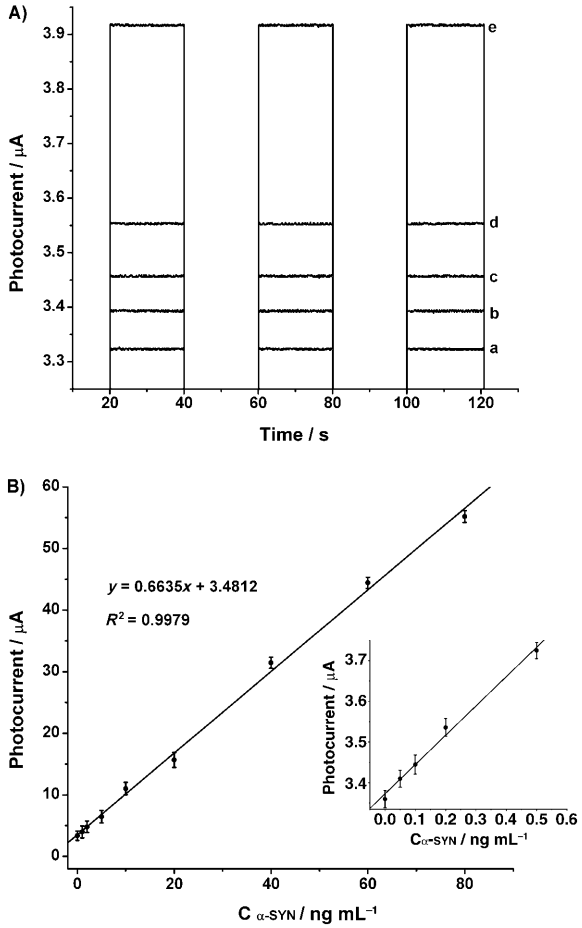

Figure 9. A) The photocurrent response of the TiO_2-Au-Ab_1-α-SYN-{Ab_2-Au-GOx} immunosensor in the presence of a) 0, b) 0.05, c) 0.1, d) 0.2, e) 0.5 ng mL^{-1} α-SYN. The excitation light was switched on and off as indicated. B) Calibration plot corresponding to the photocurrent of the TiO_2-Au-Ab_1-α-SYN-{Ab_2-Au-GOx} immunosensor. The inset is the amplification of the linear range from 0.05 to 0.5 ng mL^{-1} for α-SYN determination.

immunosensor in the presence of different concentrations of α-SYN. It can be seen that the rise and fall of the photocurrent corresponds well to the irradiation being switched on and off. As the concentration of α-SYN increased, the photocurrent response enhanced accordingly. Figure 9B shows representative photocurrent data obtained from the immunosensors incubated with various concentrations of α-SYN. The linear relationship between the photocurrent response and the α-SYN concentration was observed in a range from 50 pg mL^{-1} to 100 ng mL^{-1} with a correlation coefficient of 0.9979. The detection limit of this method was estimated to be 34 pg mL^{-1}, based on 3 sd/m, in which sd is the standard deviation of the measurements of noncomplementary target solutions and m is the slope of the plot in Figure 9B. The results illustrate the successful development of the Au-doped TiO_2 photoelectrochemical immunosensor. In addition to Au-doped TiO_2 nanotubes serving as arrays for effective antibody immobilization, the {Ab_2-Au-GOx} bioconjugates could remarkably improve the sensitivity of the immunosensor, and the detection limit compared favorably with the value of 2.5 μg mL^{-1} obtained from an enzyme-linked immunosorbent assay.[40]

Conclusion

A novel and sensitive photoelectrochemical immunosensor based on Au-TiO_2 nanotube arrays was fabricated for the detection of α-synuclein (α-SYN). The Au-TiO_2 nanotube arrays played an essential role in not only the immobilization of the protein molecules, but also the photocurrent generation during the assay process. The secondary antibody and glucose oxidase could be easily bound to the Au nanoparticles to yield {Ab_2-Au-GOx} bioconjugates. Through an immunoreaction of antibody and antigen, an immunosensor with a sandwich structure (TiO_2-Au-Ab_1-α-SYN-{Ab_2-Au-GOx}) was formed. The signal amplification of the developed immunosensor was achieved by utilizing {Ab_2-Au-GOx} bioconjugates and Au-doped TiO_2 nanotubes. Results indicated that the photoelectrochemical immunosensor for α-synuclein had good performance with high sensitivity, acceptable fabrication reproducibility, and excellent stability. Moreover, the designed immunosensor opens up a new perspective for the application of photoelectrochemistry, and might be of great importance for clinical and biological analysis of a wide range of significant proteins.

Experimental Section

Chemicals and materials: Monoclonal anti-α-synuclein (Ab_1), glucose oxidase (GOx, 21.2 U mg^{-1}, type II from Aspergillus niger), bovine serum albumin (BSA), glucose, *N*-hydroxysuccinimide (NHS), 1-ethyl-3-(3-dimethylaminopropyl)carbodiimide (EDC), and mercaptoacetic acid (MACA) were all purchased from Sigma–Aldrich (St. Louis, MO, USA). Polyclonal anti-α-synuclein (Ab_2) was supplied by Santa Cruz Biotechnology, Inc. (Santa Cruz, CA, USA). Human α-synuclein (α-SYN) was obtained from Chemicon International Inc. (Temecula, CA, USA). Chloroauric acid ($HAuCl_4$) and trisodium citrate were obtained from China National Medicines Corporation Ltd. (China). Disodium hydrogen phosphate, potassium dihydrogen phosphate, and hydrofluoric acid were purchased from Shanghai Chemical Reagent Co. (China). Pieces of pure titanium foil (dimensions: 15 mm × 4 mm × 0.5 mm) were purchased from Tite Inc. (Shanghai, China). The 0.01 and 0.05 M phosphate buffer solutions (PBS) were prepared by using Na_2HPO_4 and KH_2PO_4. All solutions were prepared using Milli-Q (Millipore, Bedford, MA, USA) A-10 gradient (18 MΩ cm) deionized water.

Apparatus and instruments: Electrochemical experiments were achieved with a CHI 660C electrochemical system (CH Instruments, Austin, TX, USA). A three-electrode system comprising a prepared immunosensor as working electrode, a platinum wire as auxiliary electrode, and Ag/AgCl (3 M KCl) as reference electrode was employed for all chemical experiments. The scanning electron micrographs were recorded with a scanning electron microscope (SEM, S-4800, Hitachi Instrument, Japan). The TEM images were performed by using transmission electron microscopy (JEOL Model JEM 2100, Japan). Light absorption was measured using a UV-visible spectrophotometer (model Cary 50, Varian Corp., USA). An 8 W UV lamp with central wavelength of 365 nm was used as the light source.

Fabrication of Au-TiO_2 nanotubes: The electrochemical anodic oxidation technique was used to fabricate the highly ordered TiO_2 nanotube array electrode.[41] Prior to anodization, the titanium foils were first mechanically polished with different abrasive papers and rinsed in an ultrasonic bath of cold distilled water for 10 min. Then the cleaned titanium foils were soaked in a mixture of HF and HNO_3 acids for 1 min (the mixing ratio of HF/HNO_3/H_2O was 1:4:5 in volume). After the Ti foils had been rinsed with acetone and deionized water for 10 min they were dried in air at room temperature. The TiO_2 nanotube electrode was fabricated in a cylindrical electrochemical reactor (radius 30 mm and height about 70 mm). Hydrofluoric acid (0.5 wt%) was used as the electrolyte, and a platinum electrode served as the cathode during the whole process. A potential of 20 V was used in this experiment. Anodized titanium foils were annealed in a dry oxygen environment at 500 °C for 1 h; heating and cooling rates were kept at 2.5 °C min^{-1}.

A novel photoelectrochemical deposition method was exploited to modify the resulting nanotubes with Au nanoparticles. The TiO_2 nanotubes served as the working electrode in a conventional photoelectrochemical cell. An Ag/AgCl (3 M KCl) electrode and a platinum electrode served as the reference and counter electrode, respectively. The photoelectrochemical deposition of Au nanoparticles was carried out by cyclic voltammetry with a potential range from 0.0 to +1.4 V for 30 min under the irradiation of light at 365 nm wavelength. The photoelectroplating solution was prepared by dissolving $HAuCl_4 \cdot 3H_2O$ (0.1 mM) in H_2SO_4 solution (0.5 M).

Preparation of the {Ab_2-Au-GOx} bioconjugates: Au nanoparticles were prepared according to the previous protocol by adding a trisodium citrate solution to a boiling $HAuCl_4$ solution.[42] The resulting colloids were stored in dark bottles at 4 °C when not in use. The pH of the Au nanoparticle solution was adjusted to 9.0 with K_2CO_3 (0.2 M). The bioconjugates were freshly prepared by addition of Ab_2 (200 μg mL^{-1}, 40 μL) and GOx (6 mg mL^{-1}, 100 μL) in PBS (0.01 M, pH 7.4) to Au nanoparticles (1.0 mL). The mixture was incubated at room temperature with gentle mixing for 2 h, and then blocked by BSA solution (100 μL, 1%) for 30 min. The solution was centrifuged for 15 min at 15000 rpm, and the supernatant was removed. The nanoparticles were washed with PBS (0.01 M, pH 7.4) for further purification and separated as above. The resulting {Ab_2-Au-GOx} bioconjugates were redispersed in PBS, and were stored at 4 °C when not in use.[43] The quality of Au nanoparticles and {Ab_2-Au-GOx} bioconjugates were monitored with TEM and UV-visible spectroscopy.

Fabrication of the photoelectrochemical immunosensor: The photoelectrochemical immunosensor was fabricated on Ti foils. Scheme 1a and b depict the fabrication process of TiO_2 nanotubes and Au-TiO_2 nanotubes as described in the Experimental Section. Au-TiO_2 nanotube arrays with a 4 × 4 mm^2 surface area were used to anchor the primary antibody. First, the Au-TiO_2 was immersed in MACA aqueous solution (2 mM) for 12 h

at 4 °C (Scheme 1c). Afterward, the carboxyl groups of MACA were activated by immersing the Au-TiO_2 for 1 h in an aqueous solution containing EDC (2 mM) and NHS (5 mM), followed by rinsing with deionized water. Then, the activated electrode was immersed into a mixture of Ab_1 solution (5 μL) for 1 h to yield the TiO_2-Au-Ab_1 electrode (Scheme 1d). The resulting electrode was washed with PBS (0.01 M, pH 7.4), and then blocked with BSA (10 μL, 1.5 %) for 1 h at room temperature. Thereafter, 5 μL of various concentrations of target α-SYN samples were applied to the TiO_2-Au-Ab_1 electrodes for 1 h at room temperature (Scheme 1e). For the binding reaction between antibody and antigen, the electrodes were immersed in {Ab_2-Au-GOx} bioconjugate solution (5 μL) for an incubation period of 1 h (Scheme 1f). Finally, the obtained electrodes were washed thoroughly with PBS to remove nonspecifically bound conjugates, and then stored at 4 °C prior to use.

Photoelectrochemical measurements: All photoelectrochemical measurements were carried out in a standard three-electrode system using a CHI660C electrochemical system. The prepared immunosensor acted as a working electrode, Ag/AgCl (3 M KCl) as a reference electrode, and a Pt wire as a counter electrode. The applied potential was +0.6 V. The photocurrent measurements were performed in a home-built experimental system containing PBS (2.0 mL, pH 7.0) at room temperature. The 8 W UV lamp used as a light source irradiated the Au-TiO_2 nanotubes from the front side. After the background photocurrent was stabilized, the response was subsequently recorded as the excitation light was turned on and off.

Acknowledgements

This work was financially supported by the National Natural Science Foundation of China (20775026, 21075041, 30772523), Science and Technology Commission of Shanghai Municipality (no. 1052nm06500), "Shu Guang Project" of Shanghai Municipal Education Commission, P.R. China (05SG30).

[1] C. G. Goetz, in *Parkinson's Disease Diagnosis and Clinical Management* (Eds: S. Factor, W. Weiner), Demos Medical Publishing, New York, **2002**, p. 19.
[2] D.-C. Wu, P. Teismann, K. Tieu, M. Vila, V. Jackson-Lewis, H. Ischiropoulos, S. Przedborski, *Proc. Natl. Acad. Sci. USA* **2003**, *100*, 6145–6150.
[3] C. E. H. Moussa, C. Wersinger, Y. Tomita, A. Sidhu, *Biochemistry* **2004**, *43*, 5539–5550.
[4] C. Follmer, L. Romão, C. M. Einsiedler, T. C. R. Porto, F. A. Lara, M. Moncores, G. Weissmüller, H. A. Lashuel, P. Lansbury, V. M. Neto, J. L. Silva, D. Foguel, *Biochemistry* **2007**, *46*, 472–482.
[5] M. B. Feany, W. W. Bender, *Nature* **2000**, *404*, 394–398.
[6] E. Masliah, E. Rockenstein, I. Veinbergs, M. Mallory, M. Hashimoto, A. Takeda, Y. Sagara, A. Sisk, L. Mucke, *Science* **2000**, *287*, 1265–1269.
[7] J. Xu, S. Kao, F. J. S. Lee, W. Song, L. Jin, B. A. Yankner, *Nat. Med.* **2002**, *8*, 600–606.
[8] J. Liu, Y. Zhou, Y. Wang, H. Fong, T. M. Murray, J. Zhang, *J. Proteome Res.* **2007**, *6*, 3614–3627.
[9] E. Lee, H. Cho, C. Lee, D. Lee, K. C. Chung, S. R. Paik, *Biochemistry* **2004**, *43*, 3704–3715.
[10] C. Li, E. A. Lutz, K. M. Slade, R. A. S. Ruf, G. Wang, G. J. Pielak, *Biochemistry* **2009**, *48*, 8578–8584.
[11] K. D. Volkova, V. B. Kovalska, G. M. Segers-Nolten, G. Veldhuis, V. Subramaniam, S. M. Yarmoluk, *Biotech. Histochem.* **2009**, *84*, 55–61.
[12] A. Rekas, C. G Adda, J. Andrew Aquilina, K. J. Barnham, M. Sunde, D. Galatis, N. A. Williamson, C. L. Masters, R. F. Anders, C. V. Robinson, R. Cappai, J. A. Carver, *J. Mol. Biol.* **2004**, *340*, 1167–1183.
[13] V. Mani, B. V. Chikkaveeraiah, V. Patel, J. S. Gutkind, J. F. Rusling, *ACS Nano* **2009**, *3*, 585–594.
[14] G. Liu, Y. Lin, J. Wang, H. Wu, C. M. Wai, Y. Lin, *Anal. Chem.* **2007**, *79*, 7644–7653.
[15] C. J. McNeil, D. Athey, W. On Ho, *Biosens. Bioelectron.* **1995**, *10*, 75–83.
[16] C. Duan, M. E. Meyerhoff, *Anal. Chem.* **1994**, *66*, 1369–1377.
[17] C. G. Bauer, A. V. Eremenko, E. Ehrentreich-Forster, F. F. Bier, A. Makower, H. B. Halsall, W. R. Heineman, F. W. Scheller, *Anal. Chem.* **1996**, *68*, 2453–2458.
[18] J. Wang, P. V. A. Pamidi, K. R. Rogers, *Anal. Chem.* **1998**, *70*, 1171–1175.
[19] R. Yuan, D. Tang, Y. Chai, X. Zhong, Y. Liu, J. Dai, *Langmuir* **2004**, *20*, 7240–7245.
[20] R. E. Ionescu, C. Gondran, L. A. Gheber, S. Cosnier, R. S. Marks, *Anal. Chem.* **2004**, *76*, 6808–6813.
[21] F. Darain, D. S. Park, J. Park, S. Chang, Y. Shim, *Biosens. Bioelectron.* **2005**, *20*, 1780–1787.
[22] M. Kanungo, D. N. Srivastava, A. Kumar, A. Q. Contractor, *Chem. Commun.* **2002**, 680–681.
[23] G. Wang, P. Yu, J. Xu, H. Chen, *J. Phys. Chem. C* **2009**, *113*, 11142–11148.
[24] M. Liang, S. Liu, M. Wei, L. Guo, *Anal. Chem.* **2006**, *78*, 621–623.
[25] V. Pardo-Yissar, E. Katz, J. Wasserman, I. Willner, *J. Am. Chem. Soc.* **2003**, *125*, 622–623.
[26] D. Dong, D. Zheng, F. Wang, X. Yang, N. Wang, Y. Li, L. Guo, J. Cheng, *Anal. Chem.* **2004**, *76*, 499–501.
[27] W. Tremel, *Angew. Chem.* **1999**, *111*, 2311–2315; *Angew. Chem. Int. Ed.* **1999**, *38*, 2175–2179.
[28] R. Wang, C. Ruan, D. Kanayeva, K. Lassiter, Y. Li, *Nano Lett.* **2008**, *8*, 2625–2631.
[29] D. Chen, G. Wang, J. Li, *J. Phys. Chem. C* **2007**, *111*, 2351–2367.
[30] S. Liu, A. Chen, *Langmuir* **2005**, *21*, 8409–8413.…
[31] A. K. M. Kafi, G. Wu, A. Chen, *Biosens. Bioelectron.* **2008**, *24*, 566–571.
[32] N. Chandrasekharan, P. V. Kamat, *J. Phys. Chem. B* **2000**, *104*, 10851–10857.
[33] H. Li, Z. Bian, J. Zhu, Y. Huo, H. Li, Y. Lu, *J. Am. Chem. Soc.* **2007**, *129*, 4538–4539.
[34] N. Zhou, J. Wang, T. Chen, Z. Yu, G. Li, *Anal. Chem.* **2006**, *78*, 5227–5230.
[35] S. Phadtare, A. Kumar, V. P. Vinod, C. Dash, D. V. Palaskar, M. Rao, P. G. Shukla, S. Sivaram, M. Sastry, *Chem. Mater.* **2003**, *15*, 1944–1949.
[36] C. M. Stoscheck, *Methods Enzymol.* **1990**, *182*, 50–68.
[37] A. Ambrosi, M. T. Castañeda, A. J. Killard, M. R. Smyth, S. Alegret, A. Merkoçi, *Anal. Chem.* **2007**, *79*, 5232–5240.
[38] Y. Chen, C. Yu, T. Cheng, W. Tseng, *Langmuir* **2008**, *24*, 3654–3660.
[39] A. Hoffman, E. Carraway, M. Hoffmann, *Environ. Sci. Technol.* **1994**, *28*, 776–785.
[40] A. W. Fjorback, K. Varming, P. H. Jensen, *Scand. J. Clin. Lab. Invest.* **2007**, *67*, 431–435.
[41] W. Zhu, Y. An, X. Luo, F. Wang, J. Zheng, L. Tang, Q. Wang, Z. Zhang, W. Zhang, L. Jin, *Chem. Commun.* **2009**, 2682–2684.
[42] B. V. Enustun, J. Turkevich, *J. Am. Chem. Soc.* **1963**, *85*, 3317–3328.
[43] S. Bi, Y. Yan, X. Yang, S. Zhang, *Chem. Eur. J.* **2009**, *15*, 4704–4709.

Received: June 11, 2010
Published online: October 29, 2010

